9

High Resolution Magnetic Imaging by Local Tunneling Magnetoresistance

W. Wulfhekel

An introduction to spin-polarized scanning tunneling microscopy with a soft magnetic tip is given. After illustrating the fundamental physical effect of tunneling magnetoresistance and giving a short historical background, it is shown how magnetic and topographic information can be separated using a modulation technique of the tip magnetization. Important for the functionality of the method is to avoid magnetostriction in the tip during reversal of its magnetization. It is shown that this is theoretically and experimentally possible with an appropriate tip material of very low magnetostriction. The closure domain structure of Co(0001) is studied and ultrasharp 20° domain walls of only 1.1 nm width are found. This narrow width is explained on the basis of a micromagnetic model, and a lateral resolution of the technique better than 1 nm is shown. The limits of the technique due to the stray field of the magnetic tip are illustrated. In the case that the stray field of the tip influences the sample under investigation, the local magnetic susceptibility can be measured. Furthermore, we focus on the contrast mechanism and give evidence that the tunneling magnetoresistance depends on the barrier height in agreement with Slonczewski's model. Finally, the possibility of magnetic imaging through a non-magnetic overlayer is discussed.

9.1 Introduction

Since the invention of scanning tunneling microscopy (STM) in 1981 by Binning and Rohrer [1], the technique has developed into an invaluably powerful surface analysis tool due to its real space imaging capabilities with atomic resolution [2]. Working in the field of magnetic imaging, one may ask the simple question: Is it possible to develop a technique similar to STM to image magnetic domains with high resolution? The invention of spin-polarized scanning tunneling microscopy (SP-STM) is the direct answer to this question. In an SP-STM not only is the electron charge used to map the surface topography, but also the electron spin is utilized to image the spin structure of the sample, which is directly related to the sample magnetization. The principle of operation of an SP-STM is based on a fundamental property of ferromagnets. Due to the spin-sensitive exchange interaction between localized electrons

(Heisenberg model) or electrons in a delocalized electron gas (Stoner model), the electronic density of states splits up into different minority and majority densities (Fig. 9.1a). This is in contrast to paramagnetic substances, where the distributions of spin-up and spin-down electrons are identical. It was Jullière [3] who discovered in 1975 the consequences of this imbalance of majority and minority electrons, i.e., the spin polarization, on tunneling between two ferromagnets. In his fundamental experiment, two magnetic films, Fe and Co, were isolated by a thin Ge film to form a tunnel junction. The two magnetic films had the same easy axis of magnetization but different coercive fields. This permitted the alignment of their magnetization parallel or antiparallel as a function of an applied magnetic field. Jullière found that the tunneling conductance G depends on the relative orientation of the magnetization of the two layers. For parallel orientation, the conductance G was 14% higher than for antiparallel orientation. He explained his finding with the spin polarization of the tunneling electrons. Under the assumption of a small bias voltage across the junction and in the absence of spin-flip scattering during the tunneling process, the electrons in the ferromagnets near the Fermi energy determine the tunneling conductance of the junction. For a parallel orientation, the majority/minority electrons of the first electrode tunnel into the majority/minority states in the second electrode, respectively, as depicted in Fig. 9.1a. In the simple case that the transmission through the barrier material itself shows no spin dependence, the conductance $G_{\uparrow\uparrow}$ is proportional to the density N of initial and final states and hence is proportional to the product of the initial and final majority and minority densities:

$$G_{\uparrow\uparrow} \propto N_{\uparrow}(1)N_{\uparrow}(2) + N_{\downarrow}(1)N_{\downarrow}(2) \tag{9.1}$$

For antiparallel orientation of the magnetization (see Fig. 9.1b), majority/minority electrons tunnel into minority/majority states and the conductance $G_{\uparrow\downarrow}$ is proportional to:

$$G_{\uparrow\downarrow} \propto N_{\uparrow}(1)N_{\downarrow}(2) + N_{\downarrow}(1)N_{\uparrow}(2)\ . \tag{9.2}$$

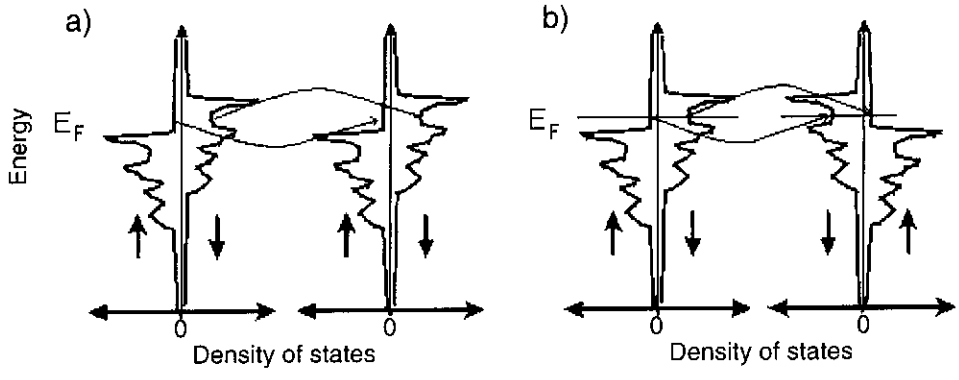

Fig. 9.1. Schematic drawing of spin-conserved tunneling between two ferromagnetic materials represented by their density of states. In (**a**) the two ferromagnets are magnetized parallel such that majority electrons from one electrode tunnel into minority states of the other electrode, while in (**b**) the ferromagnets are magnetized antiparallel such that majority electrons from one electrode tunnel into minority states of the other

With the spin polarization $P_i = (N_\uparrow(i) - N_\downarrow(i))/(N_\uparrow(i) + N_\downarrow(i))$ of the electrons of electrode i, the relative variation of the conductance is given by:

$$\Delta G/G_{\uparrow\uparrow} = 2P_1P_2/(1 + P_1P_2) \; . \tag{9.3}$$

This variation of the conductance and consequently of the resistance is called the tunneling magnetoresistance (TMR). More than a decade later, Slonczewski treated the problem of spin-polarized tunneling rigorously in the free electron model [4]. Neglecting higher order spin effects like spin accumulation, he calculated the dependence of the conductance on the angle θ between the magnetization of the two layers:

$$G = G_0(1 + P_1'P_2'\cos\theta) \; . \tag{9.4}$$

Where P_i' is the effective spin-polarization of the combination of ferromagnet i and the barrier, while G_0 is the mean conductance containing no parameters of the magnetization direction of the layers. The $\cos\theta$ dependence is strict, since it originates from the quantum mechanical rotation behavior of the spin $1/2$ tunneling electrons, i.e., it reflects the electron spin. Later, Slonczewski's prediction for the angular dependence of the TMR effect was also experimentally confirmed [5].

During the last decade, many attempts have been made to use the TMR effect in an STM to obtain spin sensitivity. Two different approaches have been of major importance: First, the use of ferromagnetic tips that lead to a spin-polarized tunneling according to Jullière's model discussed above, and, secondly, the use of GaAs tips with spin-polarized carriers that are created by optical pumping with circularly polarized light [6]. Early attempts in the beginning of the 1990s to use ferromagnetic tips and utilize the TMR effect were of limited success. The experiments by Johnson and Clarke [7], who used bulk Ni tips to image the magnetic structure of surfaces in air, were dominated by spurious effects like magnetostriction and mechanical vibrations of the tip or sample. Almost at the same time, Wiesendanger et al. [8] reported spin-polarized vacuum tunneling at room temperature between a ferromagnetic CrO_2 tip and the topological antiferromagnetic Cr(001) surface [9]. Using a tungsten tip, topographic constant current line scans revealed atomic steps on Cr(001) of the expected step height of 0.14 nm, while using a ferromagnetic CrO_2 tip, alternating step heights of 0.16 and 0.12 nm were observed. This was attributed to the TMR effect between the ferromagnetic tip and the ferromagnetically ordered Cr atoms on the terraces. When the spin polarization of the tip and the Cr terrace atoms are parallel, the tunneling current is enhanced due to the TMR effect (see Eq. 9.4) and in the constant current mode of the STM, the tip is retracted by a small amount (0.02 nm). On the adjacent atomic terrace on Cr, the spin polarization of the terrace atoms is opposite due to the topological antiferromagnetic order of Cr(001) [9]. Therefore, on this terrace, the TMR effect leads to a reduction of the current and the STM tip approaches. This mechanism results in alternating step heights seen with a spin polarized tip. However, no separation of topography and spin information could be obtained in this approach, and reference measurements had to be acquired with nonmagnetic tips.

In the mid-1990s, a more promising approach for magnetic imaging using optically pumped GaAs tips in combination with a lock-in technique to separate topographic and magnetic information was established [10–12]. By using circularly polarized light, spin polarized carriers are excited into the conduction band of the tip and then tunnel into the sample. The spin polarization of the electrons can be selected by the helicity of the light [6]. This is the key to separating spin information from topographic information. By modulating the helicity of the light, and by this the spin polarization of the carriers, modulations in the tunneling current are induced due to spin-dependent tunneling. The modulations were detected with a lock-in amplifier. The signal is used to construct magnetic images, as shown in Fig. 9.2. Hence, the modulation of spin polarization enables one to separate spin information (Fig. 9.2a) from topographic information (Fig. 9.2b), although only one physical parameter, i.e., the tunneling current, is measured. The spin information is contained in the AC part of the tunneling current at the frequency of the optical modulation, while the topographic information is contained in the DC component. This optical modulation technique, however, suffers from a rather low contrast. Further, an unintended additional magneto-optical contrast of limited lateral resolution is present due to the interaction of the light and the sample [13]. Only a few studies on domain patterns have been published using this technique, and no experiments have been presented

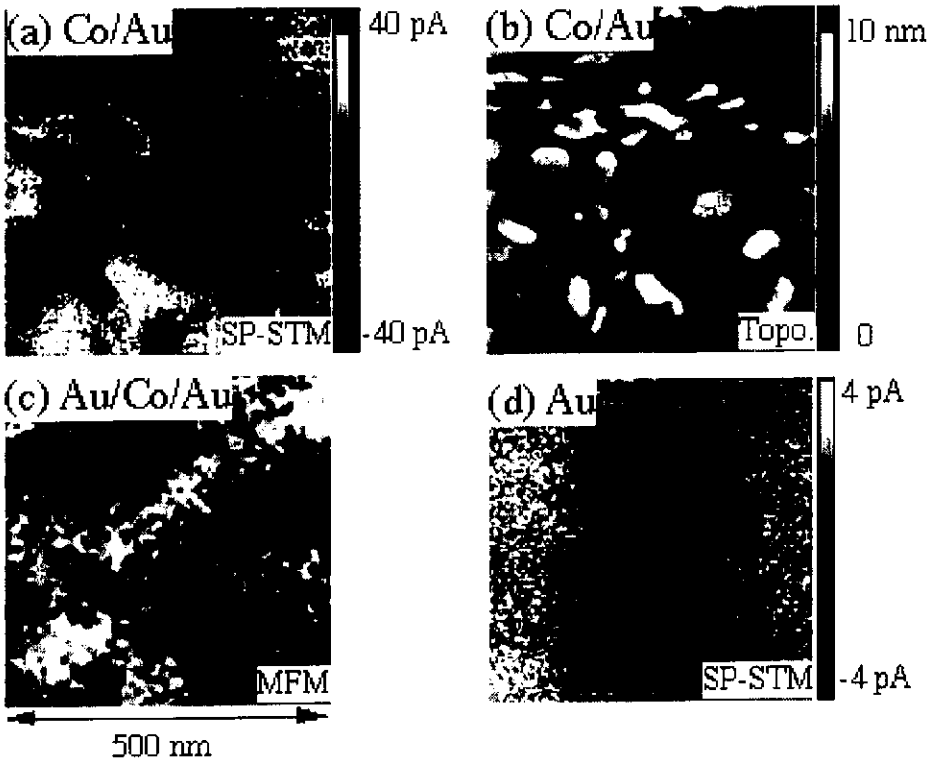

Fig. 9.2. (**a**) Magnetic SP-STM image and (**b**) topographic image of the same location of a Co film on Au. The polarization image shows magnetic domains that are similar to those obtained by MFM on a Au-covered sample depicted in (**c**). Magnetic SP-STM image of an Au film showing a non-vanishing contrast. All images are 0.5 × 0.5 μm. Figure taken from [14]

that rigorously prove the magnetic origin of the observed domains. Moreover, non-magnetic films are reported to show in some cases a considerable signal (see Fig. 9.2c) similar to the domains in magnetic films [14], raising questions about the reliability of this method.

Recently, different groups revived the first approach, the use of ferromagnetic tips. In these new approaches, spin and topographic information could be separated by two methods [15, 16]. Bode et al. used spin-polarized scanning tunneling spectroscopy to obtain spin information. This approach is described in detail in Chap. 10. The second method is addressed in the following section.

9.2 Experimental Setup

In this section, we focus on the use of ferromagnetic tips in combination with a modulation technique of the spin polarization. Analogous to the concept of optically pumped GaAs tips, a modulation of the spin polarization is used to separate spin information from topographic information in the tunneling current. In this approach to SP-STM, a soft magnetic tip is chosen as the STM tip. The longitudinal magnetization of the tip is switched periodically with the frequency f by the magnetic field induced by a small coil wound around the tip, as depicted in Fig. 9.3. The whole volume of the tip is ferromagnetic such that the reversal of the whole tip is driven by the field of the coil at the backside of the tip, and the apex is switched between the two energetically favored longitudinal magnetized states, as will be discussed in detail below. In this way, the spin polarization of the electrons at the tip apex is periodically reversed. Magnetic contrast is separated from the topographic information by phase-sensitive detection of the Fourier component of frequency f via a lock-in amplifier. Due to the local tunneling magnetoresistance effect between the magnetic tip and the surface of the specimen, the tunneling current shows an AC component related to the spin polarization of the sample. If the switching frequency f of the tip is chosen well above the cut-off frequency of the feedback loop of the STM, the variations in the tunneling current are not compensated by the current feedback loop and may be detected in the tunneling current with the lock-in amplifier. The DC component in the tunneling current is used to map the topography simultaneously with the spin structure. Important for the functionality of the method is that mechanical vibrations are avoided during the switching process of the tip and that the tip–sample distance is kept constant. Primarily, this is necessary to prevent the tip from crashing into the sample surface, since it is positioned only a few Å in front of the sample during STM operation. Secondly, one has to avoid changes in the tunneling current due to distance changes in order not to cover the small modulations of the tunneling current caused by the tunneling magnetoresistance. Due to the exponential dependence of the tunneling current on the gap width, the tolerable changes of the distance are only on the order of 0.05 Å. For larger mechanical vibrations, the variations in the tunneling current are larger than those caused by the TMR effect, which under favorable conditions is in the range of several 10% [17]. To achieve this low level of mechanical vibrations during the switching of the tip magnetization,

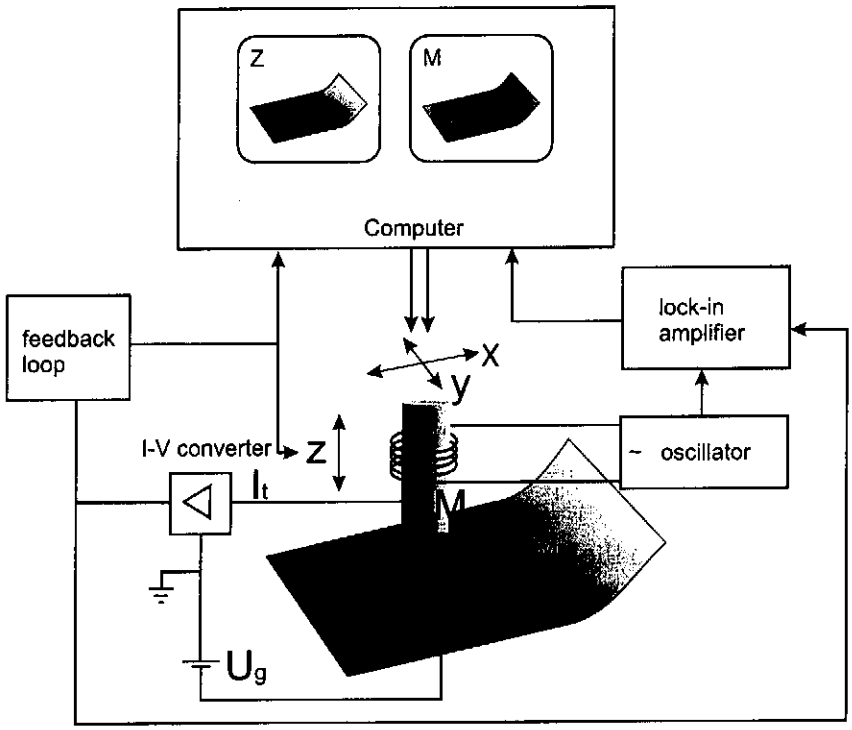

Fig. 9.3. Schematic drawing of the experimental setup. The magnetic tip of the STM can be scanned in x and y directions over the surface, while the z component is regulated with a constant current feedback loop such that the tip follows the topography of the sample. During scanning, the tip is periodically switched by the magnetic field of a coil wound around the tip. The resulting variations of the tunneling current are detected after preamplification with a lock-in amplifier to construct the magnetic image of the surface

special care has to be taken in the choice of the tip material. For optimal performance, one needs low coercive fields of the material to minimize magnetic dipolar forces between the tip and the exciting coil. Furthermore, a vanishing magnetostriction of the tip material prevents changes in the tip length during switching. Magnetization losses should be low to avoid energy dissipation and thus periodic heating and thermal expansion of the tip. Best results were obtained with an amorphous metallic glass of the CoFeSiB family with high Co concentration [18]. The material offers extremely low coercivities in the range of 50 μT with very high initial magnetic susceptibility, negligible magnetostriction ($< 4 \times 10^{-8}$) [19] and a low saturation magnetization of 0.5 T combined with low magnetization losses at frequencies up to 100 kHz.

The magnetic tips were electrochemically etched from specially designed thin CoFeSiB wires of 130 μm diameter. As etching agent, a dilute mixture of HCl and HF was used that was suspended by surface tension as a thin liquid membrane in a Pt ring during etching. The pH value was tuned such that the formation of silica from the Si in the amorphous wire was prevented. Using low etching currents on the order of 250 μA, sharp and pointed tips were created, as can be seen in Fig. 9.4a. The cone angle of the tip is typically between 8 and 15°, and the radius of curvature can be as low as 20 nm. These tips were then fixed with conducting glue to a nonmagnetic tip

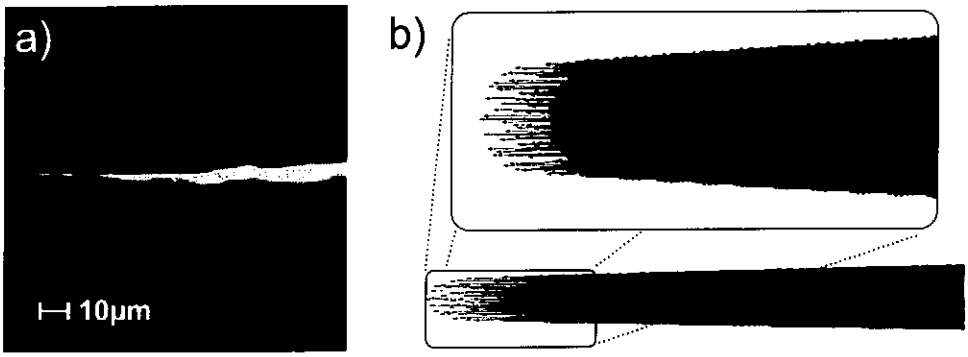

Fig. 9.4. (**a**) Scanning electron microscopy image of an etched CoFeSiB tip, (**b**) micromagnetic simulation of the tip magnetization. The inset shows the apex of the tip in higher magnification. The total length of the tip is 500 nm

shaft, around which the magnetic coil was wound. The coil was mechanically fixed to the shaft by insulating glue to avoid vibrations. The coil, which is used to switch the longitudinal magnetization of the tip, is sufficiently light, such that it can be scanned together with the tip during imaging of the surfaces.

9.3 Magnetic Switching and Magnetostriction of the Tip

To understand which magnetic information can be obtained with the soft magnetic tips, the magnetic configuration of the tip and its switching behavior were investigated. Micromagnetic calculations of the end of the tip were carried out to find the stable domain configuration. The simulations have been performed with a micro magnetic finite element algorithm based on direct energy minimization. The shape of the tip is approximated by a cone of an aperture angle of 12°, capped at its end with a hemisphere of 30 nm diameter. Since the whole magnetic tip is too large to be modeled in the framework of numerical micromagnetism, we analyzed only the last 500 nm of the end of the tip. This length, however, is well above the single domain particle diameter such that the end of the tip is free to form domains in the volume that is included in the simulations. As the stable configuration, we found the single domain state with a homogeneous magnetization pointing along the axis of the tip (see Fig. 9.4b) in agreement with what one would expect for an elongated object. The apex of the tip is free from vortices. On the outer surface of the cone-shaped tip, the magnetization points along the axis of the tip and hence does not lie in the surface of the tip. This can be explained by the limited saturation magnetization of the tip material. If the magnetization of the tip followed the contours of the cone, all the flux of the tip would be concentrated at the tip apex, where the flux would exceed the saturation of the material. However, the magnetization of the material is limited by the saturation magnetization, and the flux leaks out of the tip. This leaking keeps the magnetization exactly along the tip axis on the outer surface of the cone-shaped tip. Due to symmetry, the configuration of magnetization opposite than that depicted in Fig. 9.4b has the same energy. There are two stable configurations, and, therefore,

the end of the tip shows a bistable behavior. The switching of the magnetization of the tip is a more complex process. As has been shown using Kerr microscopy, the wires show a multidomain structure on the millimeter scale and lack a single, large Barckhausen jump [20]. Nevertheless, due to their extreme magnetic softness, they exhibit a high magnetic susceptibility. As a consequence, when a magnetic field is applied with the small coil at the backside of the tip, the flux created is dragged into the needle-shaped tip. Applying a field below saturation results in a movement of the internal 180° domain walls such that the flux induced by the coil at the backside is fully kept inside the tip. Magnetostatically, it is unfavorable for the flux to leak out at the side of the tip and instead it is guided to the apex. It is then only the direction of the flux that determines which of the two single domain configurations of the end of the tip is the more stable one. If pinning of domain walls does not hinder switching of the end of the tip, it is efficiently switched between the two states just by the collected flux from the backside of the tip. We confirmed this switching behavior of the tip by micromagnetic simulations that revealed no energetic barrier for domain wall motion in the vicinity of the tip apex and showed complete switching between two states of opposite longitudinal magnetization. In this way, sensitivity for the perpendicular component of the sample magnetization is achieved with our SP-STM. The simulations of the switching process also give an estimate of the expected magnetostriction of the tip during the process of switching. As switching of the tip proceeds by domain wall formation and movement and not by coherent rotation of the entire magnetization of the tip, magnetostriction is active in the magnetic domain walls only. Thereby, the length of the tip is changed by the magnetostriction in the wall, when it exits (or enters) the apex of the tip. The width of an 180° domain wall at the end of the tip is around 20 nm, as the micromagnetic calculations show. Together with the low magnetostriction constant of the material of $< 4 \times 10^{-8}$ this results in an undetectable distance change on the order of 10^{-5} Å. Theoretically, vibration due to magnetostriction can safely be neglected.

We checked experimentally for magnetostriction and other mechanical vibrations of the tip by performing test measurements of the SP-STM setup on a nonmagnetic Cu(001) sample. Figure 9.5a displays the topography of a Cu(001) crystal as obtained with a CoFeSiB tip while applying an alternating field of about 1 mT at 20 kHz. Terraces separated by atomic steps are clearly visible. Obviously, vibrations due to magnetostriction or other effects are small enough to get stable STM images. Note that the weak vibrations visible as ripples in the topography are not related to the switching of the tip, but are due to insufficient damping of vibrations of the building. In the signal obtained from the lock-in amplifier, however, one observes a weak contrast at the step edges (see Fig. 9.5b). This cross talk from the topography is on the order of 0.3% of the tunneling current and is due to small mechanical vibrations of the tip caused, e.g., by eddy currents acting on the tip in the alternating field of the coil. These vibrations can be avoided when the exciting field is reduced by one order of magnitude (see Fig. 9.5c and d). The lock-in signal using an exciting field of 100 μT is zero and does not show any crosstalk from the topography while the magnetization of the end of the tip is still switched, as will be discussed below. Hence, vibrations due to magnetostriction can be excluded down to the sensitivity

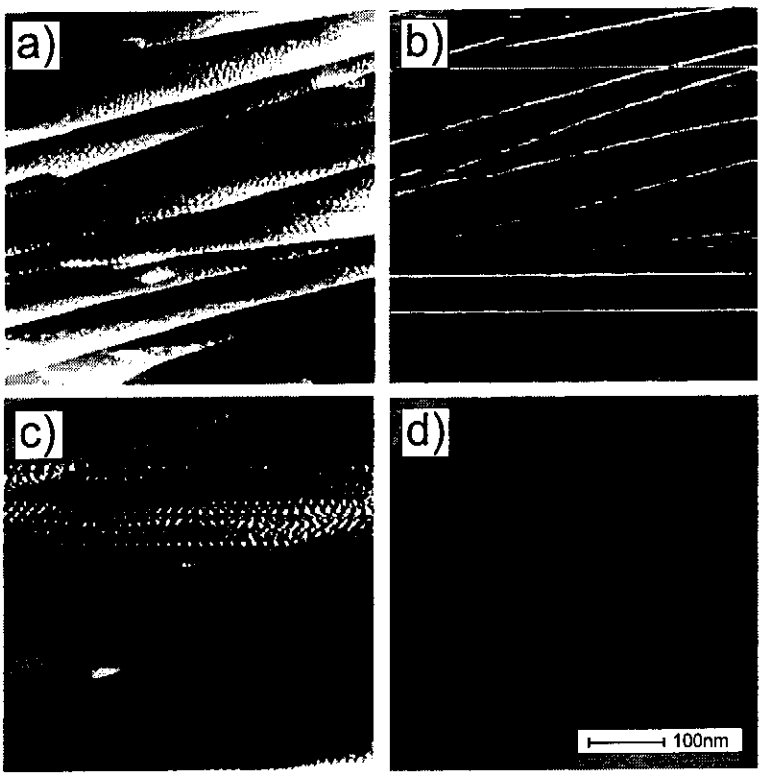

Fig. 9.5. (**a**), (**c**) STM scans of the topography and (**b**), (**d**) the spin signal of the same areas of Cu(001). During scanning an alternating magnetic field of 20 kHz was created by the coil around the tip. (**a**), (**b**) The field was set at 1.1 mT and (**c**), (**d**) 100 μT. For the higher field, mechanical vibrations of the tip are observed causing a cross-talk from the topography into the spin signal. (**b**), (**d**) Both spin images are normalized to a black and white contrast corresponding to 0.3% of the tunneling current

of the lock-in detection of $< 0.1\%$ of the tunneling current. Taking the well-known exponential dependence of the tunneling current on distance [21], one can estimate the vibrations in the narrow frequency bands around the modulation frequency f and its second harmonic. The lock-in signals correspond to distance changes between tip and sample of less than 5×10^{-4} Å, i.e., mechanical vibrations of the tip due to magnetostriction or other forces can experimentally be neglected. Using CoFeSiB, it is feasible to measure the tunneling magnetoresistance locally between the tip and the sample without unwanted mechanical vibrations.

9.4 Magnetic Imaging of Ferromagnets

Since the magnetic contrast of the SP-STM is based on the tunneling magnetoresistance effect, i.e., an interface effect, the instrument is mostly sensitive to the topmost atomic layer of the sample. As a consequence, atomically clean sample surfaces are required. The same holds for the apex of the tip. Therefore, the SP-STM experiments have to be performed in ultrahigh vacuum. After transferring new tips to the STM, the magnetic tips have to be cleaned in-situ by sputtering with 1 keV

Ar^+ ions to remove the native oxide at the apex. Samples were cleaned by cycles of argon sputtering (1 keV) and annealing until no traces of contamination could be found in Auger electron spectra. After sample and tip preparation, tunneling images of the topography, as well as the magnetization were recorded simultaneously at room temperature. After the initial tests for vibrations on a nonmagnetic substrate, we focused on imaging ferromagnetic surfaces. As a first example, a polished but polycrystalline Ni disk is imaged. On large scans (several μm^2) of the Ni surface, strong magnetic contrasts can be found in the spin signal, as displayed in Fig. 9.6a. The image of the spin signal shows two regions, i.e., domains with different intensities, separated by a fine, bright line, i.e., a domain wall. The observed domains in the spin signal are not related to the topography, as can be seen by comparing the topography of Fig. 9.6b with the spin signal of the very same area (white box in Fig. 9.6a). This excludes the possibility that the observed domains are caused by a crosstalk from the topography. In agreement with the theoretically predicted bistable behavior of the tip, the domains in the spin signal disappear abruptly when the size of the exciting field is lowered below 40 μT and reappear for fields above 50 μT. Upon further increase of the field, the contrast in the domain images does not rise further. The width of the domain walls observed on the polycrystalline Ni disk is between 100 and 150 nm and hence in qualitative agreement with calculated wall widths of 85–200 nm, depending on the wall type and the crystal orientation of Ni [22]. This gives a first hint of the good lateral magnetic resolution. The domains in the spin signal, however, are changing on the time scale of hours during repeated scanning, pointing at an influence of the magnetic tip on the observed domains. This might be attributed to the magnetically soft nature of polycrystalline Ni.

To learn more about SP-STM, its capabilities and limitations, a better defined surface than polycrystalline Ni was chosen for further studies. The (0001) surface of

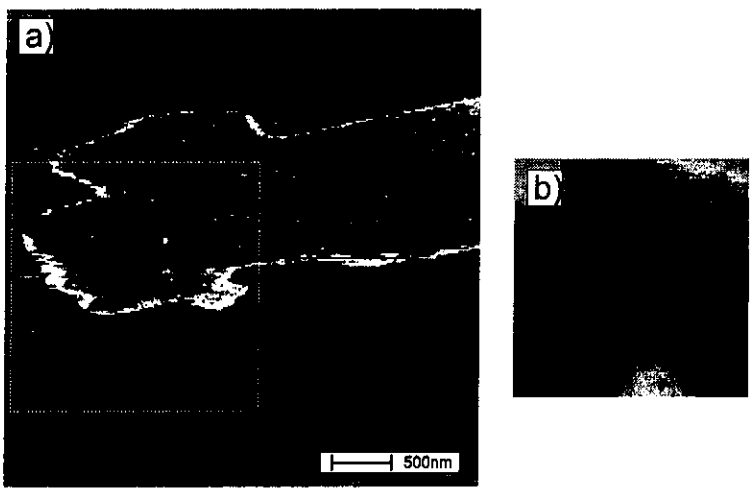

Fig. 9.6. (**a**) SP-STM scans of the spin structure of a polished polycrystalline Ni surface. To show that the observed spin contrast is not related to the morphology, the topography (**b**) and the spin signal (white box in (**a**)) of the very same area were recorded. The black-white contrast in the spin signal is 0.5% of the tunneling current. The peak-to-peak roughness of the topography corresponding to full black-white contrast is 3 nm